
Guessing Smart: Biased Sampling for Efficient Black-box Adversarial Attacks

Thomas Brunner^{1,2} Frederik Diehl^{1,2} Michael Truong Le^{1,2} Alois Knoll²

Abstract

We consider adversarial examples in the black-box decision-based scenario. Here, an attacker has access to the final classification of a model, but not its parameters or softmax outputs. Most attacks for this scenario are based either on transferability, which is unreliable, or random sampling, which is often slow. Focusing on the latter, we propose to improve the efficiency of sampling-based attacks with prior beliefs about the target domain. We identify two such priors, image frequency and surrogate gradients, and discuss how to integrate them into a unified sampling procedure. We then formulate the *Biased Boundary Attack*, which achieves a drastic speedup over the original Boundary Attack. We demonstrate the effectiveness of our approach against an ImageNet classifier. We also showcase a targeted attack for the Google Cloud Vision API, where we craft convincing examples with just a few hundred queries. Finally, we demonstrate that our approach outperforms the state of the art when facing strong defenses: Our attack scored second place in the targeted attack track of the *NeurIPS 2018 Adversarial Vision Challenge*.

1. Introduction

Ever since the term was first coined, adversarial examples have enjoyed much attention from Machine Learning researchers. The fact that tiny perturbations can lead otherwise robust-seeming models to misclassify an input could pose a major problem for safety and security. But when discussing adversarial examples, it is often unclear how realistic the scenario of a proposed attack truly is. In this work, we consider a threat setting with the following parameters:

Black-box. The black-box setting assumes that the attacker has access only to the input and output of a model. Compared to the white-box setting, where the attacker has com-

plete access to the architecture and parameters of the DNN model, attacks in this setting are significantly harder to conduct: Most state-of-the-art white-box attacks (Goodfellow et al., 2015; Carlini & Wagner, 2017; Madry et al., 2018) rely on gradients that are directly computed from the model parameters, which are not available in the black-box setting.

Decision-based classification (label-only). Depending on the output format of the DNN, the problem of missing gradients can be circumvented. In a score-based scenario, the model provides real-valued outputs (for example, softmax activations). By applying tiny modifications to the input, an attacker can estimate gradients by observing changes in the output (Chen et al., 2017) and then follow this estimate to generate adversarial examples. The decision-based setting, in contrast, provides only a single discrete result (e.g. the top-1 label), and gradient estimation is not possible. Searching for adversarial examples now becomes a combinatorial problem that is much harder to optimize (Brendel et al., 2018a).

Limited queries. Black-box attacks in the real world might not be feasible if they need thousands of queries to the model, and possibly multiple hours' time, to be successful. We therefore consider a scenario where the attacker must find a convincing adversarial example in less than 1000 queries.

Targeted. An untargeted attack is considered successful when the classification result is any label other than the original. Depending on the number and semantics of the classes, it can be easy to find a label that requires little change, but is considered adversarial (e.g. egyptian cat vs persian cat). A targeted attack, in contrast, needs to produce exactly the specified label. This task is strictly harder than the untargeted attack, further decreasing the probability of success.

In this setting, current state-of-the-art attacks are either unreliable or inefficient. Our contribution is as follows:

- We introduce the *Biased Boundary Attack* (BBA), which uses prior beliefs about the target domain to sample adversarial perturbations with a high probability of success.
- We discuss low-frequency patterns and projected gra-

¹fortiss GmbH, Munich, Germany ²Department of Informatics, Technical University of Munich, Germany. Correspondence to: Thomas Brunner <brunner@fortiss.org>.

dients as biases for the sampling procedure.

- We show that our method outperforms the previous state of the art in few-query black box attacks and present our winning submission to the NeurIPS 2018 Adversarial Vision Challenge. We have released the full source of our implementation¹.

2. Related Work

There currently exist two major schools of attacks in the threat setting we consider:

2.1. Transfer-based

It is well known that adversarial examples display a high degree of transferability, even between different model architectures (Tramèr et al., 2017). Transfer attacks seek to exploit this by training substitute models that are reasonably similar to the model under attack, and then apply regular white-box attacks to them.

Typically this is performed by iterative applications of fast gradient-based methods, such as the Fast Gradient Sign Method (FGSM) (Goodfellow et al., 2015) and, more generally, Projected Gradient Descent (PGD) (Madry et al., 2018). The black-box model is used in the forward pass, while the backward pass is performed with the surrogate model (Athalye et al., 2018a). In order to maximize the chance of a successful transfer, newer methods use large ensembles of substitute models, and applying adversarial training to the substitute models has been found to increase the probability of finding strong adversarial examples even further (Tramèr et al., 2018).

Although these methods currently form the state of the art in label-only black-box attacks (Kurakin et al., 2018), they have one major weakness: as soon as a defender manages to reduce transferability, direct transfer attacks often run a risk of complete failure, delivering no result even after thousands of iterations. As a result, conducting transfer attacks is a cat-and-mouse game between attacker and defender, where the attacker must go to great lengths to train models that are just as robust as the defender’s. Therefore, transfer-based attacks can be very efficient, but also somewhat unreliable.

2.2. Sampling-based

Circumventing this problem, sampling-based attacks do not rely on direct transfer and instead try to find adversarial examples by randomly sampling perturbations from the input space.

Perhaps the simplest attack consists of sampling a hyper-

¹https://github.com/ttbrunner/biased_boundary_attack_avc

sphere around the original image, and drawing more and more samples until an adversarial example is found. Owing to the high dimensionality of the input space, this method is very inefficient and has been dismissed as completely unviable (Szegedy et al., 2014). While this is not our main focus, our results in Section 4 show that even this crude attack can be accelerated and made competitive with existing black-box attacks.

Recently, a more sophisticated attack has been proposed: the Boundary Attack (BA) (Brendel et al., 2018a). This attack is initialized with an input of the desired class, and then takes small steps along the decision boundary to reduce the distance to the original input. Previous works have established that regions which contain adversarial examples often have the shape of a “cone” (Tramèr et al., 2018), which can be traversed from start to finish. At each step, the Boundary attack employs random sampling to find a sideways direction that leads deeper into this cone. From there, it can then take the next step towards the target.

The Boundary Attack has been shown to be very powerful, producing adversarial examples that are competitive with even the results of state-of-the-art white-box attacks (Brendel et al., 2018a). However, its achilles heel is query efficiency: to achieve these results, the attack typically needs to query the model hundreds of thousands of times.

Score-based attacks (Chen et al., 2017; Tu et al., 2018; Ilyas et al., 2018) also use random sampling and have recently received much attention, however they do not target our setting where scores are not available. Ilyas et al. propose an interesting variant of their attack, successfully applying gradient estimation to discrete labels. Although this does fit our scenario, it is still very inefficient (see section 4).

Therefore, sampling-based attacks are very flexible, but often too inefficient for practical use.

3. The Biased Boundary Attack

Most current sampling-based attacks have one thing in common: they draw samples from either normal or uniform distributions. This means that they perform unbiased sampling, perturbing each input feature independently of the others. But this can be very inefficient, especially against a strong defender.

Consider the distribution of natural images: adjacent pixels are typically not independent of each other, but often have similar colors. This alone is a strong indicator that drawing perturbations from i.i.d random variables will lead to adversarial examples that are clearly out of distribution for natural image datasets. This, of course, renders them vulnerable to detection and filtering.

It seems only logical to constrain the search space to pertur-

bations that we believe to have a higher chance of success. Putting this concept into practice, we propose the *Biased Boundary Attack (BBA)*, which uses domain knowledge as prior beliefs for its sampling procedure, and through it achieves a large speedup over the original Boundary Attack.

In this section, we outline two such priors for the domain of image classification and show how to integrate them into a single, unified, attack.

3.1. Low-frequency perturbations

When one looks at typical adversarial examples, it quickly becomes apparent that most existing methods yield perturbations with high image frequency. But high-frequency patterns have a significant problem: they are easily identified and separated from the original image signal, and are often dampened by spatial transforms. Indeed, most of the winning defenses in the NeurIPS 2017 Adversarial Attacks and Defences Competition were based on denoising (Liao et al., 2018), simple median filters (Kurakin et al., 2018), and random transforms (Xie et al., 2018). In other words: state-of-the-art defenses are designed to filter high-frequency noise.

At the same time, we know that it is possible to synthesize "robust" adversarial examples which are not easily filtered in this way. Compare Athalye et al. (2018b): Their robust perturbations are largely invariant to filters and transforms, and - interestingly enough - at first glance seem to contain very little high-frequency noise. It seems obvious that such patterns should be ideal for breaking black-box defenses.

Inspired by this observation, we hypothesize that image frequency alone could be a key factor in robustness of adversarial perturbations. If true, then simply limiting perturbations to the low-frequency domain should increase the success chance of an attack, while incurring no extra cost.

Perlin Noise patterns. A straightforward way to generate parametrized, low-frequency patterns, is to use Perlin Noise (Perlin, 1985). Originally intended as a procedural texture generator for computer graphics, this function creates low-frequency noise patterns with a reasonably "natural" look. One such pattern can be seen in Figure 1c. But how can we use it to create a prior for the Biased Boundary Attack?

Let k be the dimensionality of the input space. The original Boundary Attack (Figure 2a) works by applying an orthogonal perturbation η^k along the surface of a hypersphere around the original image, in the hope of moving deeper into an adversarial region. From there, a step is taken towards the original image. In the default configuration, candidates for η^k are generated from samples $s \sim \mathcal{N}(0, 1)^k$, which are projected orthogonally to the source direction and normalized to the desired step size. This leads to the directions being uniformly distributed along the hypersphere.

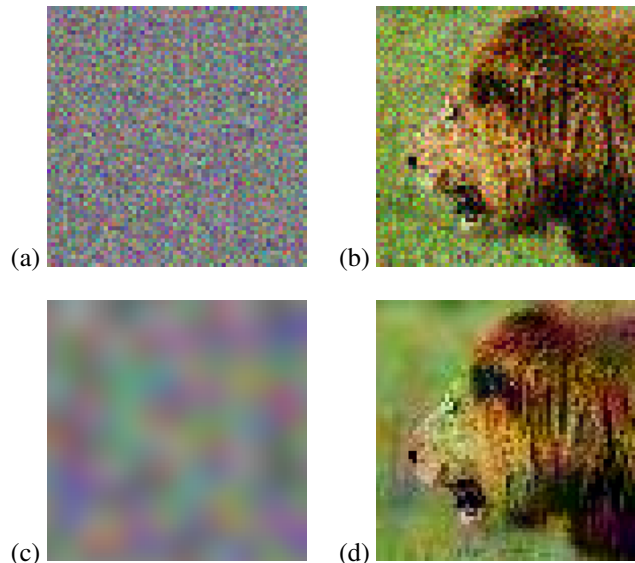


Figure 1. Adversarial perturbations for an untargeted attack, obtained after testing 1000 random samples. (a) and (b): Sampled from a normal distribution. (c) and (d): Sampled from a distribution of Perlin noise patterns. In both cases, the network misclassifies the image, and picks a different label than the original (lion).

To introduce a low-frequency prior into the Biased Boundary Attack, we instead sample from a distribution of Perlin noise patterns (Figure 2b). Perlin noise is typically parametrized with a permutation vector v of size 256, which we randomly shuffle on every call. Effectively, this allows us to sample two-dimensional noise patterns $s \sim \text{Perlin}_{h,w}(v)$, where h and w are the image dimensions (and $h \cdot w = k$). As a result, the samples are now strongly concentrated in low-frequency regions.

Our experiments in Section 4 show that this greatly improves the efficiency of the attack. Therefore, we reason that the distribution of Perlin noise patterns contains a higher concentration of adversarial directions than the normal distribution.

Other low-frequency patterns. We note that, concurrently to our work, a similar effect has very recently been described by Guo et al. (2018). They decompose random perturbations with the Discrete Cosine Transform, and then remove high frequencies from the spectrum. Reaching the same conclusions, they go on to modify the Boundary Attack and show a large increase in efficiency. Their method was not known to us at the time of our submission to the Adversarial Vision Challenge, but we include them in our comparison on ImageNet (see section 4.2).

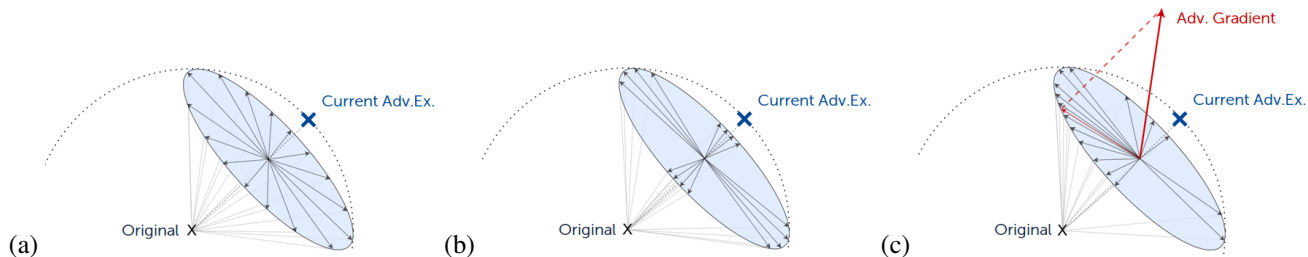


Figure 2. Sampling directions for the orthogonal step. (a) Boundary Attack: uniformly distributed along the surface of the hypersphere. (b) BBA with Perlin bias: high sample density in the direction of low-frequency perturbations. (c) BBA with Perlin and gradient biases: samples further concentrate towards the direction of the projected gradient.

3.2. Gradients from surrogate models

What other source of information contains strong hints about directions that are likely to point to an adversarial region? The natural answer is: gradients from a substitute model. A large range of such models is available to us, as many state-of-the-art black-box attacks rely on them to perform a transfer attack via PGD methods (Tramèr et al., 2018; Kurakin et al., 2018).

Arguably, the main weakness of gradient-based transfer attacks is that they fail when adversarial regions of the surrogate model do not closely match the defender’s. However, even when this is the case, those regions may still be reasonably nearby. Based on this intuition, some approaches extend gradient-based attacks with limited regional sampling (Athalye et al., 2018a). Here, we do exactly the opposite and extend a sampling-based attack with adversarial gradients. This has the significant advantage that, in the case of limited transferability, our method merely experiences a slowdown, whereas PGD-based methods often fail altogether.

Our method works as follows:

- An adversarial gradient from a surrogate model is calculated. Since the current position is already adversarial, it can be helpful to move a small distance towards the original image first, making sure to calculate the gradient from inside a non-adversarial region.
- The gradient usually points away from the target, therefore we project it onto the surface of a hypersphere around the target, as shown in Figure 2c.
- This projection is on the same hyperplane as the candidates for the orthogonal step. We can now bias the candidate perturbations toward the projected gradient by any method of our choosing. Provided all vectors are normalized, we opt for a simple addition:

$$\eta_{biased}^k = (1-w) \cdot \eta^k + w \cdot \eta_{PG}^k; \quad \eta_{biased}^k = \frac{\eta_{biased}^k}{\|\eta_{biased}^k\|}$$

- w controls the strength of the bias and is a hyperparameter that should be tuned according to the performance of our substitute model. High values for w should be used when transferability is high, and vice versa. Were we to choose the maximum value, $w = 1$, then the orthogonal step would be equivalent to an iteration of the PGD attack. In our experience, $w \leq 0.5$ generally leads to good performance.

As a result, samples concentrate in the vicinity of the projected gradient, but still cover the rest of the search space (albeit with lower resolution). In this way, substitute models are purely optional to our attack, instead of forming the central part. It should be noted though that at least *some* measure of transferability should exist. Otherwise, the gradient will point in a bogus direction and using a high value for w would reduce efficiency instead of improving it.

For the time being, this does not pose a major problem. To the best of our knowledge, no strategies exist that successfully eliminate transferability altogether. As we go on to show, even a very simple substitute model delivers a substantial speedup. In the Adversarial Vision Challenge, our attack outperforms most competitors, even though our surrogate models are much simpler than theirs.

4. Evaluation

We evaluate our approach in three steps: First, we present a range of experiments and our winning submission to the NeurIPS 2018 Adversarial Vision Challenge. Next, we attack an ImageNet classifier and compare our results to other proposed Black-box attacks. Finally, we mount an attack against the Google Cloud Vision API and show that our method is efficient against real-world commercial systems.

4.1. Adversarial Vision Challenge

When evaluating adversarial attacks and defenses, it is hard to obtain meaningful results. Very often, attacks are tested against weak defenses and vice versa, and results are cherry-picked. We sidestep this problem by instead submitting our

approach to the Adversarial Vision Challenge (AVC), where our method is pitted against state-of-the-art robust models and black-box defenses.

Evaluation setting. The AVC is an open competition between image classifiers and adversarial attacks in an iterative black-box decision-based setting (Brendel et al., 2018b). Participants can choose between three tracks:

- **Robust model:** The submitted code is a robust image classifier. The goal is to maximize the ℓ^2 norm of any successful adversarial perturbation.
- **Untargeted attack:** The submitted code must find a perturbation that changes classifier output, while minimizing the ℓ^2 distance to the original image.
- **Targeted attack:** Same as above, but the classification must be changed to a specific label.

Attacks are continuously evaluated against the current top-5 robust models and vice versa. Each evaluation run consists of 200 images with a resolution of 64x64, and the attacker is allowed to query the model 1000 times for each image. The final attack score is then determined by the median ℓ^2 norm of the perturbation over all 200 images and top-5 models (lower is better).

At the time of writing, the exact methods of most model submissions were not yet published. But seeing as more than 60 teams competed in the challenge, it is reasonable to assume that the top-5 models accurately depict the state of the art in adversarial robustness. We know through personal correspondence that most winning models used variations of Ensemble Adversarial Training (Tramèr et al., 2018), while denoisers were notably absent from at least the top 3.

Dataset. The models are trained with the Tiny ImageNet dataset, which is a down-scaled version of the ImageNet classification dataset, limited to 200 classes with 500 images each. Model input consists of color images with 64x64 pixels, and the output is one of 200 labels. The evaluation is conducted with a secret hold-out set of images, which is not contained in the original dataset and unknown to participants of the challenge.

4.1.1. RANDOM GUESSING WITH LOW FREQUENCY

Before implementing the Biased Boundary Attack, we first conduct a simple experiment to demonstrate the effectiveness of Perlin noise patterns against strong defenses. Specifically, we run a random-guessing attack that samples candidates uniformly from the surface of a ℓ^2 -hypersphere with radius ϵ around the original image:

$$s \sim \mathcal{N}(0, 1)^k; x_{adv} = x_0 + \epsilon \cdot \frac{s}{\|s\|_2}$$

With a total budget of 1000 queries to the model for each image, we use binary search to reduce the sampling distance ϵ whenever an adversarial example is found. First experiments have indicated that the targeted setting may be too difficult for pure random guessing. Therefore we limit this experiment to the untargeted attack track, where the probability of randomly sampling *any of 199* adversarial labels is reasonably high.

We add a second attack, replacing the distribution with normalized Perlin noise:

$$s \sim \text{Perlin}_{64,64}(v); x_{adv} = x_0 + \epsilon \cdot \frac{s}{\|s\|_2}$$

We set the Perlin frequency to 5 for all attacks on Tiny ImageNet. Figure 1 shows adversarial examples from both distributions. As Table 1 shows, Perlin patterns are more efficient and the attack finds adversarial perturbations with much lower distance (63% reduction), supporting the findings independently made by Guo et al. (2018). Although intended as a dummy submission to the AVC, this attack was already strong enough for a top-10 placement in the untargeted track.

Table 1. Random guessing with low frequency (untargeted).

DISTRIBUTION	MEDIAN ℓ^2 DISTANCE
NORMAL	11.15
PERLIN NOISE (OURS)	4.28

4.1.2. BIASED BOUNDARY ATTACK

Next, we evaluate the Biased Boundary Attack in our intended setting, the targeted attack track in the AVC.

To provide a point of reference, we first implement the original Boundary Attack, and initialize it with known images from the target class. Specifically, we use the training set of Tiny ImageNet, and from all images of the target class we pick the one with the lowest distance to the source image. The Boundary Attack works, but is too slow for our setting. Compare Figure 3a, where the starting point (a butterfly) is still clearly visible after 1000 iterations.

We then implement the Biased Boundary Attack by adding our first prior, low-frequency noise (see Figure 3b). As before, we simply replace the distribution from which the attack samples the orthogonal step with Perlin patterns. As shown in Table 2, this alone decreases the median ℓ^2 distance by 25%.

Finally, we add projected gradients from a surrogate model and set the bias strength w to 0.5. This further reduces the median ℓ^2 distance by another 37%, or a total of 53% when compared with the original Boundary Attack. 1000

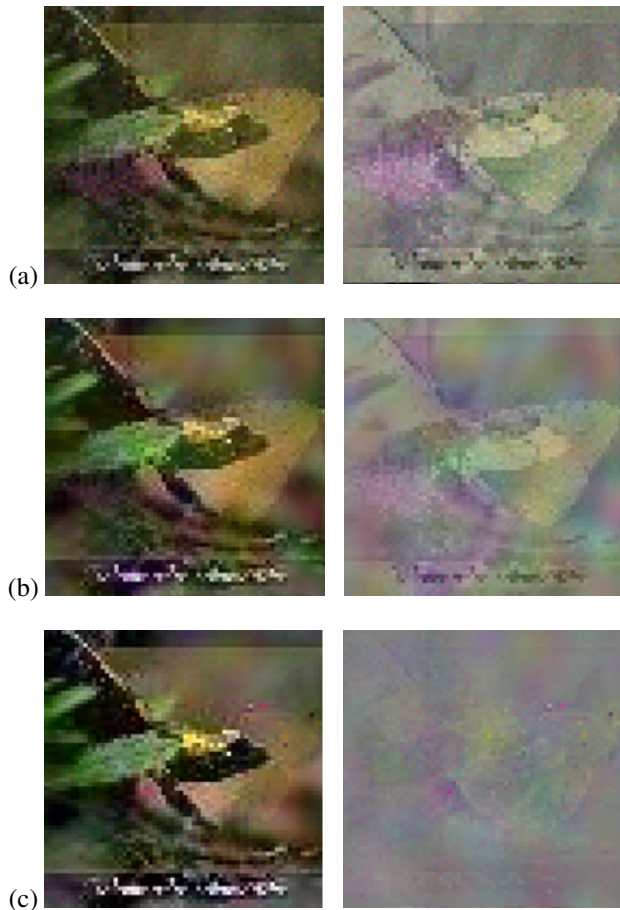


Figure 3. Comparison of Boundary Attack and Biased Boundary Attack after 1000 queries. While originally a “european fire salamander”, all three images are classified as “sulphur butterfly”. (a) Boundary Attack: $d_{\ell^2} = 9.4$ (b) BBA with Perlin bias: $d_{\ell^2} = 7.5$ (c) BBA with Perlin and projected gradient biases: $d_{\ell^2} = 4.4$. See Appendix A for more examples.

iterations are enough to make the butterfly almost invisible to the human eye (Figure 3c). See Appendix A for more adversarial examples generated on Tiny ImageNet.

In our submission to the AVC, we used an ensemble of ResNet18 and ResNet50, both of which are public baselines provided by the competition organizers. This ensemble is reasonably strong, but not state-of-the-art (the ResNet50 baseline was trained with Adversarial Logit Pairing, which has since been shown to be less effective than originally assumed (Engstrom et al., 2018; Mosbach et al., 2018)). In fact, most winning submissions to the AVC used much larger ensembles of carefully-trained models². This reinforces the claim that our method outperforms most existing attacks even when using simple surrogate models.

² See blog post at <https://medium.com/bethgelab/>

Table 2. Biases for the Boundary Attack (targeted).

ATTACK	BIAS	MEDIAN ℓ^2
BOUNDARY ATTACK	-	20.2
BBA (OURS)	PERLIN	15.1
BBA (OURS)	PERLIN + PG	9.5

4.2. Comparison on ImageNet

The AVC has shown that our attack is very efficient against strong defenses. However, we note that the dataset (Tiny ImageNet) is not in widespread use. To compare our method to established black-box attacks, we therefore implement it for an ImageNet classifier.

Setting. ImageNet consists of images with 299x299 color pixels, and has 1000 classes. We use a pre-trained InceptionV3 network (Szegedy et al., 2015), which achieves 78% top-1 accuracy. It does not employ any defenses against adversarial examples - our attack is therefore evaluated in the most common setting.

Other methods. We compare the Biased Boundary Attack to the Boundary Attack, both in its original (Brendel et al., 2018a) and low-frequency form (Guo et al., 2018). We also include approaches proposed by Ilyas et al. (2018) and Cheng et al. (2018). As an additional point of reference, we include the score-based methods ZOO (Chen et al., 2017) and AutoZOOM (Tu et al., 2018).

Evaluation. Our attack always starts with an image of the adversarial class, therefore success must be characterized by low distance to the source image. For this, we define thresholds on the ℓ^2 -norm of the adversarial perturbation, and register success when the distance is below. We create an evaluation set by randomly drawing 1000 images from the ImageNet validation set, run each attack on this set and report the average *success rate* over all images.

For the gradient bias in the BBA, we use the adversarially trained Inception-Resnet-v2 model of Tramèr et al. (2018) and set the bias strength w to 0.5. We do not perform any training ourselves. For the low-frequency bias, we set the Perlin frequency to 20.

4.2.1. UNTARGETED IMAGENET ATTACK

Arguably, untargeted attacks on ImageNet do not accurately represent a real-world scenario. After all, changing a “persian cat” to a “egyptian cat” is hardly malicious for most use cases. Nevertheless, we include this experiment since some methods (Guo et al., 2018; Cheng et al., 2018) report only untargeted results on ImageNet. We run all attacks for 4000 queries and fix the success threshold to a MSE of 0.001 ($d_{\ell^2} = 16.38$), which is the setting used by Guo et al.

Table 3. Untargeted attack on ImageNet. Results marked with (*) are reported by the respective authors, and not evaluated by us.

	SUCCESS RATE VS NUMBER OF QUERIES					
	250	500	1000	2000	4000	150 000+
BOUNDARY ATTACK	0.38	0.46	0.49	0.52	0.53	1.00 (*)
CHENG ET AL. (2018)	0.24	0.37	0.37	0.39	0.39	1.00 (*)
GUO ET AL. (2018)	0.41	0.45	0.53	0.64	0.70	-
BBA (PERLIN, OURS)	0.39	0.47	0.61	0.62	0.69	-
BBA (PERLIN + PG, OURS)	0.44	0.62	0.72	0.75	0.76	-

Discussion. Table 3 shows that our attack is successful after very few iterations, and is the most efficient by far for low query counts. It is also apparent that our low-frequency patterns are similar in performance to those of Guo et al. (2018). As an aside, our experiment sees them start with much higher success rate (41% after 250 iterations versus 9% reported by them). This is due to our choice of initialization method: Instead of adding Gaussian noise to the source image, we search the ImageNet validation set and pick the closest image to the source.

4.2.2. TARGETED IMAGENET ATTACK

We repeat the same experiment in a targeted setting over 15000 queries and fix a random target label for each example in the evaluation set (all attacks run on the same image/target combinations). Since some of the methods we compare (Ilyas et al., 2018) use ℓ^∞ distance exclusively, we set the ℓ^2 -threshold to 25.89. This corresponds to a worst-case ℓ^∞ -distortion of 0.05 if one assumes all pixels to be maximally perturbed. Appendix B shows selected examples of this evaluation.

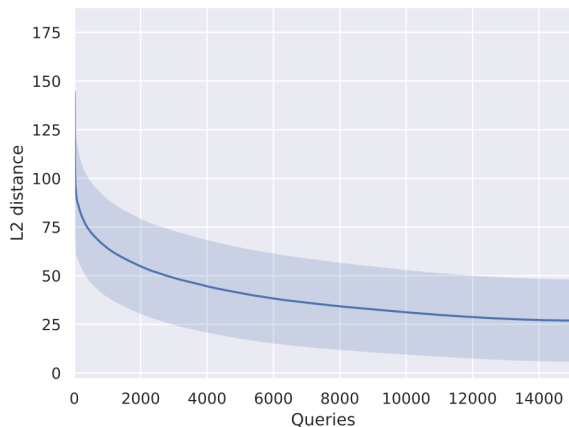


Figure 4. Query-distortion study of the targeted Biased Boundary Attack on ImageNet.

Discussion. As Figure 4 shows, our attack is very efficient below 10000 queries, but later slows down drastically. In Table 4, we see that there exist methods with higher success

rates, but they need significantly more queries to achieve them. Unfortunately, the authors do not report results at low query counts.

The only attacks that are comparable in efficiency are score-based gradient estimators. This is of little value to our setting, but it still confirms that these methods should be used whenever scores are available. Nevertheless, our evaluation shows that the BBA is the most efficient attack in a label-only few-query scenario.

4.3. Google Cloud Vision API

To show that our method can be efficient even against commercial black box classifiers, we conduct an attack against the Google Cloud Vision API. This is significantly harder than attacking ImageNet, since the exact classes are unknown. In order to craft adversarial examples in less than 1000 queries, we relax the attack formulation:

Multi-targeted attack. We have argued earlier that untargeted attacks with many redundant classes are not truly adversarial. However, the opposite is also true: to achieve an adversarial effect, it is not always necessary to target one specific class. Rather, the same effect could be achieved by targeting a group of classes - if we want to label a dog as a cat, we can take the union of all cat breeds to achieve the desired effect. This greatly simplifies the task and allows us to conduct a targeted attack against the Google Cloud Vision API with high success chance.

Turning a person into a bear. To conduct an attack with this goal, we relax the target ("bear") and formulate the adversarial criterion as:

- One of the top-3 labels must contain the word "bear" (this includes grizzly bear, brown bear, etc.)
- The words "face", "facial expression", "skin", "person" must not appear in any of the output labels.

We use the exact same implementation that we submitted to the AVC, since it is already heavily optimized. Unfortunately, this limits us to a resolution of 64x64 (see Appendix C for an experiment at ImageNet resolution).

Table 4. Targeted attack on ImageNet. The BBA is the most efficient attack in a label-only setting. However, score-based estimators still perform better if scores are indeed available. Results marked with (*) are reported by the respective authors, and not evaluated by us.

	SUCCESS RATE VS NUMBER OF QUERIES						1M+	MEDIAN QUERIES UNTIL SUCCESS
	500	1000	2500	5000	10000	15000		
<i>Label-only</i>								
ILYAS ET AL. (2018) (LABEL-ONLY)	-	-	-	-	-	-	0.9 (*)	2.7M (*)
BOUNDARY ATTACK	0.01	0.02	0.06	0.12	0.23	0.31	-	6263
BBA (PERLIN, OURS)	0.01	0.03	0.15	0.24	0.32	0.40	-	5541
BBA (PERLIN + PG, OURS)	0.05	0.08	0.14	0.27	0.50	0.63	-	3406
<i>Using confidence scores</i>								
ZOO (CHEN ET AL., 2017)	-	-	-	-	-	-	0.76 (*)	2.2M (*)
AUTOZOOM (TU ET AL., 2018)	-	-	-	-	-	0.99 (*)	-	13525 (*)
ILYAS ET AL. (2018) (GENERAL)	-	-	-	-	-	0.98 (*)	-	11550 (*)

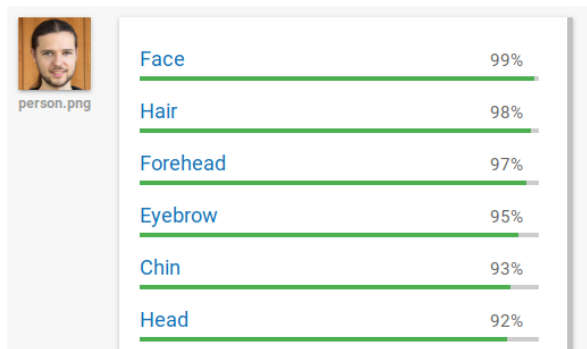


Figure 5. Clean image classified by Google Cloud Vision.



Figure 6. Adversarial image (target "bear") classified by Google Cloud Vision after 346 queries. There are no other labels, i.e. Google Cloud Vision outputs only three results. See Appendix C for more examples.

Figures 5 and 6 show the result: after only 346 iterations, our attack produces a perturbation that is still visible ($d_{\ell_2} = 5.86$), but small enough to fool an unsuspecting person. This demonstrates once more the key strength of our attack: instead of aiming for perfect adversarial examples, we achieve sufficiently good results with a very low number of queries. Again, it should be stressed that we do *not* use confidence scores (even though they are available here).

5. Conclusion

We have shown that decision-based black-box attacks can be greatly sped up by biasing their sampling procedure. The NeurIPS 2018 Adversarial Vision Challenge is testament to this: Our submission scored second place in the targeted attack track, even though our surrogate models were much simpler than those of other participants. Indeed, we expect that incorporating their models would further increase sample efficiency, and produce an even better attack as the combination of our results. We have also demonstrated that our method is competitive on ImageNet, and that it can be used to attack commercial classifiers in a very short amount of time.

And it does not end here - we have discussed only two priors for biased sampling, but there is much more domain knowledge that has not yet found its way into adversarial attacks. Other perturbation patterns, spatial transforms, adversarial blending strategies, or even intuitions about semantic features of the target class could all be integrated in a similar fashion.

With the Biased Boundary Attack, we have outlined a basic framework into which virtually any source of knowledge can be incorporated. Our current implementation crafts convincing results after very few iterations, and the threat of black-box adversarial examples becomes more realistic than ever before.

References

Athalye, A., Carlini, N., and Wagner, D. Obfuscated gradients give a false sense of security: Circumventing defenses to adversarial examples. In *Proceedings of the 35th International Conference on Machine Learning, ICML, 2018a*.

Athalye, A., Engstrom, L., Ilyas, A., and Kwok, K. Synthesizing robust adversarial examples. In *Proceedings of*

- the 35th International Conference on Machine Learning, ICML, 2018b.*
- Brendel, W., Rauber, J., and Bethge, M. Decision-based adversarial attacks: Reliable attacks against black-box machine learning models. In *International Conference on Learning Representations*, 2018a.
- Brendel, W., Rauber, J., Kurakin, A., Papernot, N., Velicki, B., Salathé, M., Mohanty, S. P., and Bethge, M. Adversarial vision challenge. *arXiv preprint arXiv:1808.01976*, 2018b.
- Carlini, N. and Wagner, D. Towards evaluating the robustness of neural networks. In *2017 IEEE Symposium on Security and Privacy (SP)*, pp. 39–57. IEEE, 2017.
- Chen, P.-Y., Zhang, H., Sharma, Y., Yi, J., and Hsieh, C.-J. Zoo: Zeroth order optimization based black-box attacks to deep neural networks without training substitute models. In *Proceedings of the 10th ACM Workshop on Artificial Intelligence and Security, AISec '17*, pp. 15–26, 2017.
- Cheng, M., Le, T., Chen, P.-Y., Yi, J., Zhang, H., and Hsieh, C.-J. Query-efficient hard-label black-box attack: An optimization-based approach. *arXiv preprint arXiv:1807.04457*, 2018.
- Engstrom, L., Ilyas, A., and Athalye, A. Evaluating and understanding the robustness of adversarial logit pairing. *arXiv preprint arXiv:1807.10272*, 2018.
- Goodfellow, I. J., Shlens, J., and Szegedy, C. Explaining and harnessing adversarial examples. In *International Conference on Learning Representations*, 2015.
- Guo, C., Frank, J. S., and Weinberger, K. Q. Low frequency adversarial perturbation. *arXiv preprint arXiv:1809.08758*, 2018.
- Ilyas, A., Engstrom, L., Athalye, A., and Lin, J. Black-box adversarial attacks with limited queries and information. In *Proceedings of the 35th International Conference on Machine Learning, ICML, 2018*.
- Kurakin, A., Goodfellow, I., Bengio, S., Dong, Y., Liao, F., Liang, M., Pang, T., Zhu, J., Hu, X., Xie, C., Wang, J., Zhang, Z., Ren, Z., Yuille, A., Huang, S., Zhao, Y., Zhao, Y., Han, Z., Long, J., Berdibekov, Y., Akiba, T., Tokui, S., and Abe, M. Adversarial Attacks and Defences Competition. *arXiv preprint arXiv:1804.00097*, 2018.
- Liao, F., Liang, M., Dong, Y., Pang, T., Hu, X., and Zhu, J. Defense against adversarial attacks using high-level representation guided denoiser. In *Proceedings of the IEEE Conference on Computer Vision and Pattern Recognition*, 2018.
- Madry, A., Makelov, A., Schmidt, L., Tsipras, D., and Vladu, A. Towards Deep Learning Models Resistant to Adversarial Attacks. *International Conference on Learning Representations*, 2018.
- Mosbach, M., Andriushchenko, M., Trost, T. A., Hein, M., and Klakow, D. Logit pairing methods can fool gradient-based attacks. *arXiv preprint arXiv:1810.12042*, 2018.
- Perlin, K. An image synthesizer. In *Proceedings of the 12th Annual Conference on Computer Graphics and Interactive Techniques, SIGGRAPH '85*, pp. 287–296, New York, NY, USA, 1985. ACM.
- Szegedy, C., Zaremba, W., Sutskever, I., Bruna, J., Erhan, D., Goodfellow, I., and Fergus, R. Intriguing properties of neural networks. In *International Conference on Learning Representations*, 2014.
- Szegedy, C., Vanhoucke, V., Ioffe, S., Shlens, J., and Wojna, Z. Rethinking the inception architecture for computer vision. *arXiv preprint arXiv:1512.00567*, 2015.
- Tramèr, F., Papernot, N., Goodfellow, I. J., Boneh, D., and McDaniel, P. D. The space of transferable adversarial examples. *arXiv preprint arXiv:1704.03453*, 2017.
- Tramèr, F., Kurakin, A., Papernot, N., Goodfellow, I., Boneh, D., and McDaniel, P. Ensemble adversarial training: Attacks and defenses. In *International Conference on Learning Representations*, 2018.
- Tu, C., Ting, P., Chen, P., Liu, S., Zhang, H., Yi, J., Hsieh, C., and Cheng, S. Autozoom: Autoencoder-based zeroth order optimization method for attacking black-box neural networks. *arXiv preprint arXiv:1805.11770*, 2018.
- Xie, C., Wang, J., Zhang, Z., Ren, Z., and Yuille, A. Mitigating adversarial effects through randomization. In *International Conference on Learning Representations*, 2018.

A. Adversarial Examples for Tiny ImageNet

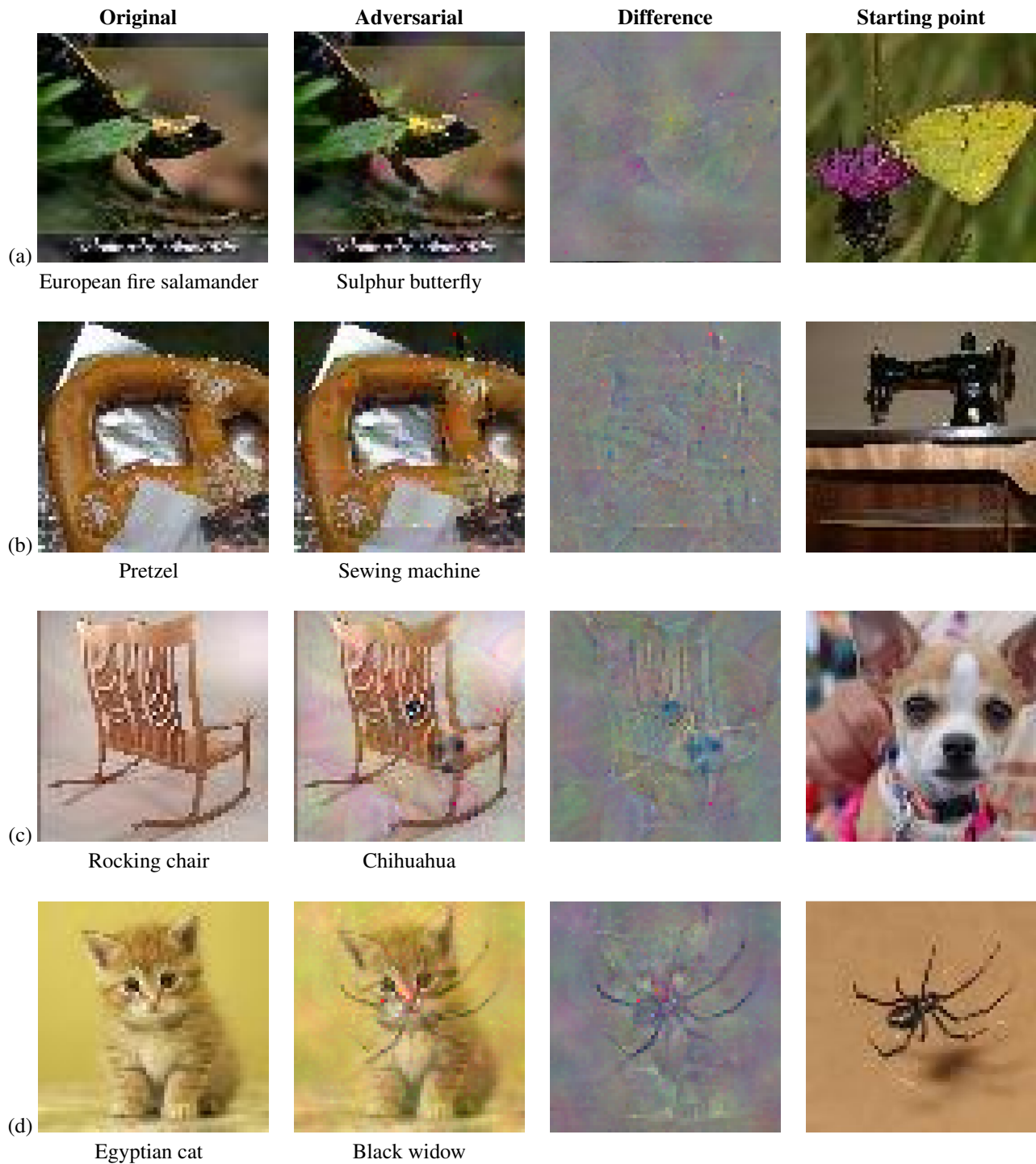


Figure 7. Targeted adversarial examples for Tiny ImageNet after 1000 queries to the model. The model being attacked is the ResNet50 baseline (ALP-trained), provided by the AVC organizers. Additionally, we preprocess model input with a denoiser and random transforms, replicating the winning defenses of the 2017 competition (Liao et al., 2018; Xie et al., 2018). In order to emulate a black-box setting, we remove ResNet50 from our surrogate, and instead use an ensemble of the ResNet18 baseline and a newly trained InceptionResnetV2. To provide an “unbiased” view of our results, (c) and (d) show limitations of our current implementation: Adversarial features are still recognizable, and more iterations are needed.

B. Adversarial Examples for ImageNet

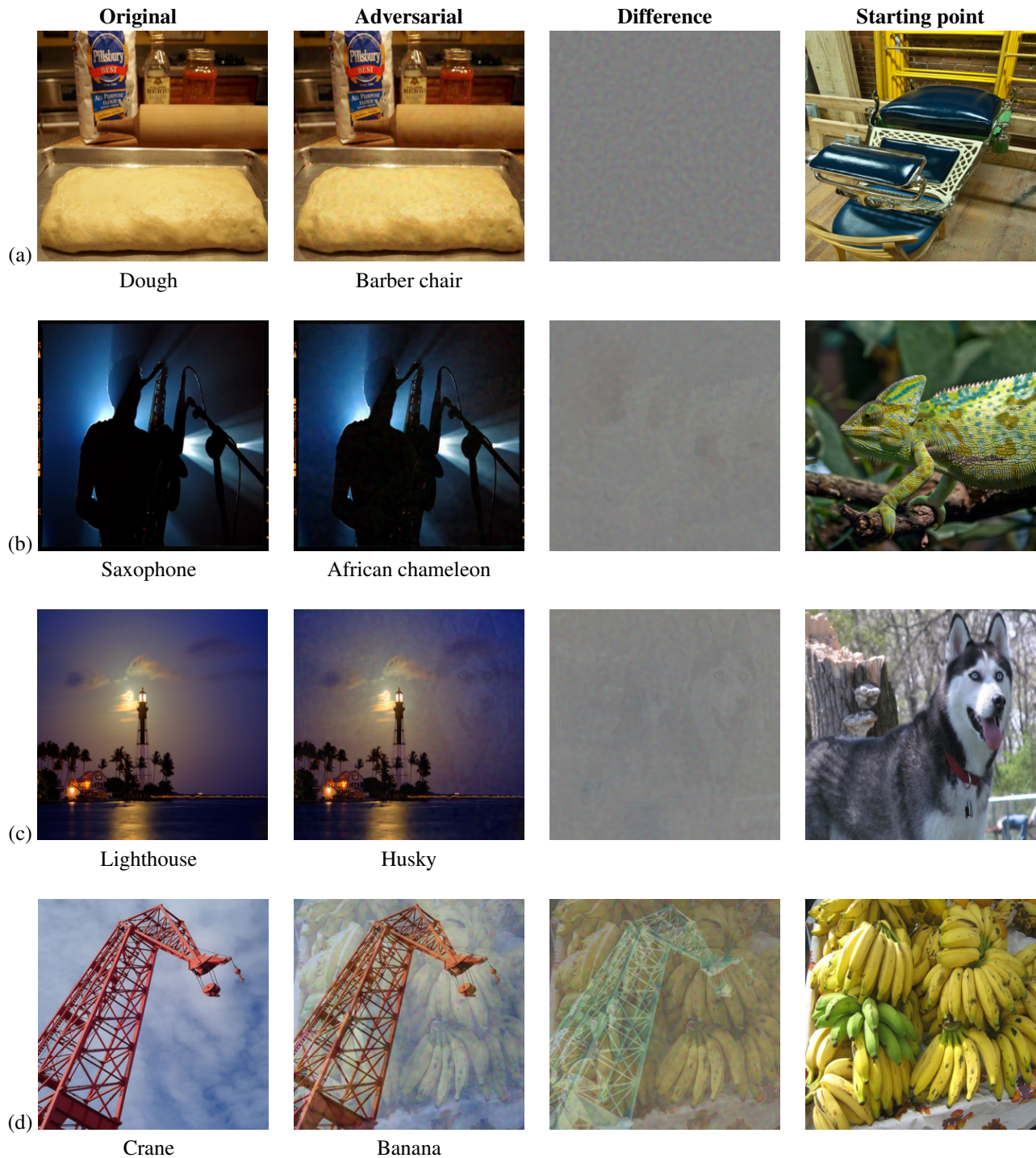


Figure 8. Targeted adversarial examples for ImageNet, generated by the Biased Boundary Attack after 15000 queries to the model. The configuration is the same as in section 4.2.2. (a-c) show successful attacks ($d_{\ell^2} < 25.89$). In (d) the attack gets stuck at $d_{\ell^2} = 52.91$ and is unsuccessful. Perhaps the most interesting is (c): Although the perturbation has a very low magnitude ($d_{\ell^2} = 9.02$), it is still clearly visible to a human observer. It is apparent that new measures for robustness are needed in order to better define "adversarial".

C. Adversarial Examples for Google Cloud Vision

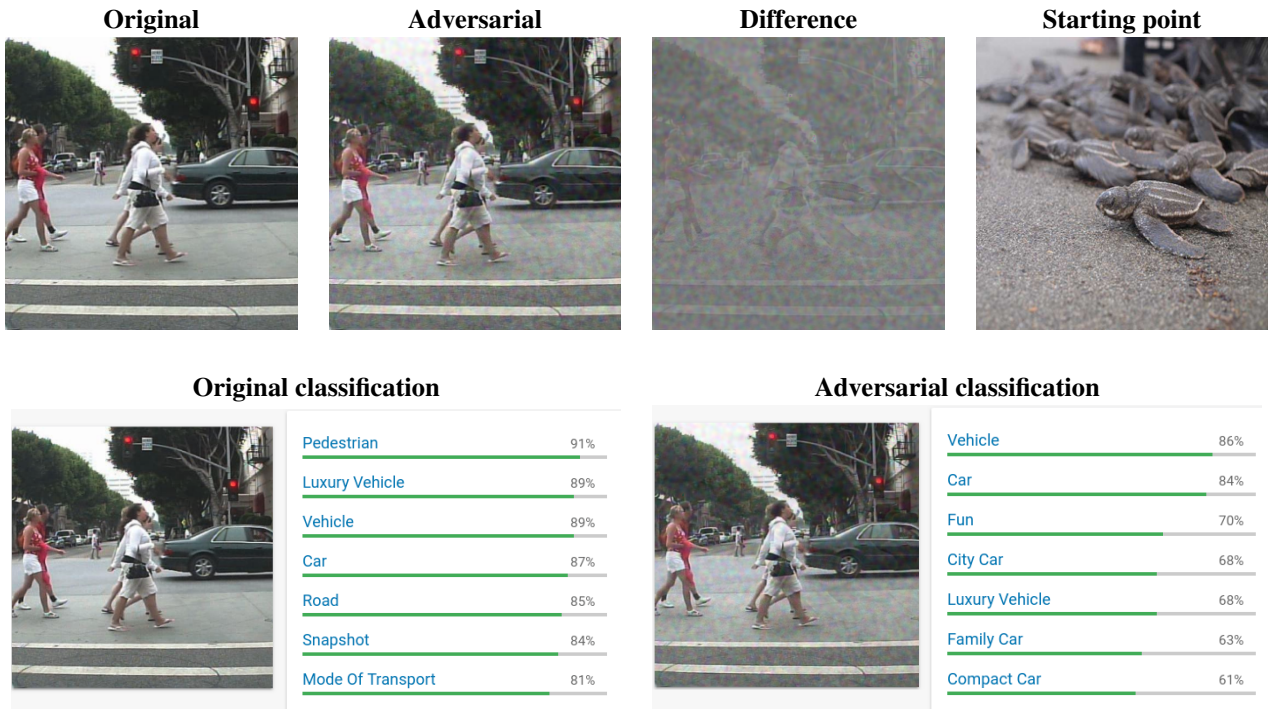


Figure 9. Adversarial example for Google Cloud Vision at ImageNet resolution, generated by the Biased Boundary Attack after 1000 queries to the API. While not invisible, the perturbation ($d_{\ell_2} = 21.52$ with resolution 299x299) might be dismissed as camera noise by an unsuspecting observer. The criterion for this example was to not only change the top-1 label, but to produce a worst-case scenario where "Pedestrian" (and all related concepts, such as "Person", "Walking", "Head", "Clothes") are removed from the prediction vector entirely. This attack could be described as *multi-untargeted*: it is harder than an untargeted attack, which is often harmless, but still easier than a completely targeted attack. Perhaps interestingly, our adversarial pattern is classified as "Fun".